

Semi-rigid connection modeling for steel frameworks

Yuxin Liu*

ACR Civil & Layout, Atomic Energy of Canada Limited (AECL), Ontario L5K 1B2, Canada

(Received October 29, 2007, Accepted February 8, 2010)

Abstract. This article provides a discussion of the mathematic modeling of connections for designing and qualifying structures, systems, and components subject to monotonic or cyclic loading. To characterize the force-deformation behavior of connections under monotonic loading, a review of the Ramberg-Osgood, Richard-Abbott, and Menegotto-Pinto models is conducted, and it is shown that these nonlinear functions can be mathematically derived by scaling up or down a linear force-deformation function. A generalized four-parameter model for simulating connection behavior is investigated to facilitate nonlinear regression analysis. In order to perform seismic analysis of frameworks, a hysteretic model accounting for loading, unloading, and reloading is described using the established monotonic model. For preliminary analysis, a method is provided to quickly determine the model parameters that fit approximately with the observed data. To reach more accurate values of the parameters, the methods of nonlinear regression analysis are investigated and the modified Levenberg-Marquardt and separable nonlinear least-square algorithms are applied in determining the model parameters. Example case studies illustrate the procedure for the computation through the use of experimental/analytical data taken from the literature. Transformation of connection curves from the three-parameter model to the four-parameter model for structural analysis is conducted based on the modeling of connections subject to fire.

Keywords: connection models; monotonic/cyclic loading; force-deformation relation; observed data; nonlinear regression analysis.

1. Introduction

It has been recognized for a long time that connection effect may significantly influence the response of the connected frameworks when beam-to-column or column-to-base connections are assumed either rigid or pinned for simplifying analysis. In most situations, a connection may be neither rigid nor pinned, and the semi-rigid (or partially restrained) behavior of the connection is required being considered in structural design (AISC 2005, CEN 2005, CSA 2009). Generally, moment-rotation connections in a frame play a more important role in resisting seismic loading compared to axial/shear connections. Recent research, however, shows that the axial/shear connections may be also important in preventing catenary failure or shear failure in extreme vertical impact loading (Liu *et al.* 2008, Liu 2009, Liu *et al.* 2010). In principle, the models discussed hereinafter can be applied for axial and/or shear connections once the corresponding analysis/test results are obtained. For example, the experimental data for single-angle all-bolted connections

*Ph.D., P. Eng., E-mail: liuyu@aecl.ca

(Gong 2009) and double-angle shear connections (Gong and Gillies 2008) may be used to establish the modelling of shear-connections. Note that more work is needed to investigate the characteristics of axial/shear failure of connections. The following discussion focuses on the modeling of moment-rotation connections, and the ways briefly described below can achieve the connection models.

First, the most straightforward way is to conduct experiments to determine the moment-rotation relationship. Many experimental results for specific connection configurations have been collected in some data banks, such as those in the literature (Goverdham 1983, Kishi and Chen 1986, Xu 1994, Kishi *et al.* 2004). To facilitate structural analysis, empirical models have been proposed using curve-fitting technique to fit these tested data. Among them the power model is the most common one being used in practice. Although the linear model (Rathbun 1936) is still used to date in the elastic analysis of frameworks because of its simplicity, nonlinear power models (Ramberg and Osgood 1943, Menegotto and Pinto 1973, Richard and Abbott 1975, Frye and Morris 1975, Lui and Chen 1986, Kishi and Chen 1986, Lee and Melchers 1986) can much more accurately simulate the behaviour of semi-rigid connections. These models are applied in the computer-based nonlinear analysis of semi-rigid frames. The parameters involved within each model were determined using linear or nonlinear regression analysis to fit with experimental measurements. Recent experience (Liu *et al.* 2008, Chen *et al.* 2010) shows that the dimensions of connection specimens in the databanks or test reports are generally less than those expected for practical frames. Thus, structural designers might have limitations to directly employ these connection data in their routine design work except the selected connections are approximately matched with those specimens described in the databanks.

Second, the way based on empirical models may be more practical, where the model parameters are determined by partial or complete theoretical analyses. For example, the three-parameter power model has been used to simulate the moment-rotation relationship of single and double web angle connections and top- and seat-angle connections (Kishi and Chen 1990). The parameters of nominal moment capacity and initial rotational stiffness were obtained by analysis, while the shape parameter was determined using the least-square curve fitting with experimental data. These parameters may be also determined using finite element method of analysis. For example, the parameters of simple power model were determined by parametrical study for extended end-plate connections (Krishnamurthy *et al.* 1979). Based on Richard-Abbott model (1975), the inelastic finite element analysis was conducted to investigate the behaviour of extended end-plate connections (Sherbourne and Bahaari 1997). Analytical results are much dependant upon the selected mechanical/mathematical models or element sizes that are used to simulate the behavior of the connected components. Since some factors such as contact between components of a connection remain unclear, the results from semi-analysis are fit with tested data but those from finite element method may be verified with experimental results.

Finally, the third way is referred to as component-based modeling of joints/connections, which can be used to directly calculate the rotational stiffness, strength and capacity of either a bolted or welded connection by analysis alone. The basic concept is taking such as column web panel in shear, column flange, bolts, end-plate, beam flange and beam web in a joint as individual components to establish an analytical model, and then the load-deformation relationship is derived based on the deformed joint in equilibrium. This method is stipulated in Eurocode 3 Part 1-8 (CEN 2005) with guidelines for designing beam-to-column, beam-to-beam, and column-to-base joints. More detailed information and application of the method are presented in the literature for modeling flush-extended-end-plate joints (Zoetemijer 1983, Simões da Silva *et al.* 2004), angle-cleat joints

(Jaspart 1997), and composite joints (Anderson 1998, Huber 2001, Barnett *et al.* 2001) for beam-to-column connections. Regarding column-to-base connections, the component-based modeling is presented in more detail in the literature (Wald 1998, Langdon and Schleyer 2004), where the moment-axial-force interaction is taken into account.

Compared to the experimental or semi-experimental method, the merit of the component-based method is that conducting analysis alone can establish the moment-rotation relationship upon using the dominant components of the joint. The analysis results can be directly incorporated in the analysis and design of simple, continuous and semi-continuous frameworks. In a framed structure, beams and columns are the basic components, and their cross-sectional properties such as moments of inertia and plastic moments are determined by pure analysis. When connections are also considered as basic components of the frame, it is logically true that calculating the connection properties such as elastic stiffness and moment capacity by analysis will facilitate the design of steel frameworks with semi-rigid connections. Note that a connection or joint is extremely localized in a structure, and the behavior of its components such as a bolt or endplate are considerably complicated. Thus, the accuracy of the component-based method might require being calibrated upon using more sophisticated analytical results and/or experimental data as performed in the research work (Baniotopoulos and Wald 2000, Simões da Silva 2008).

It is noted that the connection behavior discussed above is for the connections in the ambient environmental conditions. Temperature effects of connections on semi-rigid steel frames are crucial in the analysis accounting for fire loading. Particularly after the 911 event, the importance of designing steel structures against fire hazards is addressed in the FEMA-403 (2002) document. Testing results of steel beams in the elevating and cooling process indicate that the catenary action on beam is significant (Li and Guo 2008), and such catenary effect might be an important failure mode that causes progressive collapse through connection damage (Liu *et al.* 2010). The research results for steel connections and bolts subjected to fire (Simões da Silva *et al.* 2005, Kirby 2005) might be helpful to interpret the failure of WTC Building 7. Typical curves for moment-rotation connections in ambient temperature are shown in Fig. 1(a), while the connection curves due to elevated temperature are shown in Fig. 1(b). These curves can be obtained by either analyses or experiments. Mathematic function/s should be selected to simulate these curves, and the connection

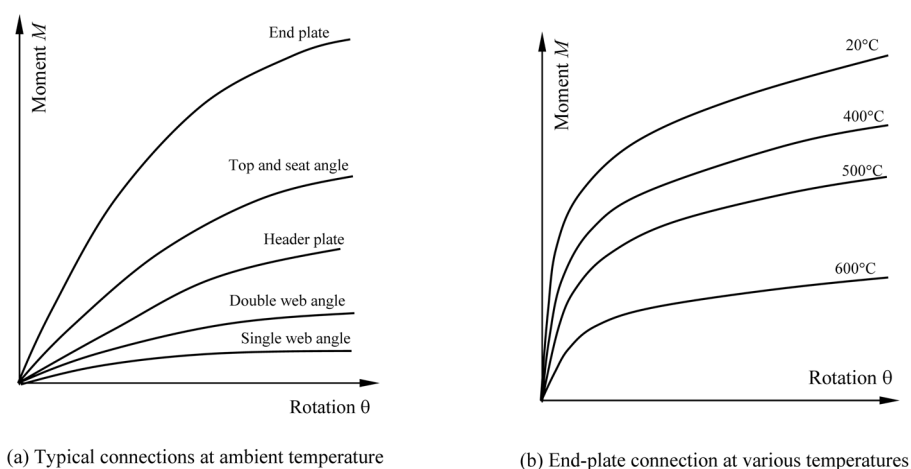


Fig. 1 Moment-rotation curves for connections

modelling is established for the purpose of structural analysis.

Once the connection models are defined by the specific parameters, these connections can be incorporated in frameworks as components like beams and columns. It should be pointed out that more advanced method of structural analysis has to be applied to predict the response of displacements and internal forces. To perform such a nonlinear structural analysis, the method applied to the progressive-collapse analysis of steel frameworks under abnormal loading may be employed (Liu *et al.* 2010), where it highlights the importance of connection behavior to bridge over local damage. When using this method, the connection stiffness should be derived using the established connection model, and the end-fixity factors should be defined to characterize the stiffness degradation behavior. In addition to the connection effect, the influence of structural stability/buckling is also included in the analysis procedure (Liu and Xu 2005, Liu *et al.* 2008). More detailed information accounting for semi-rigid connections with hybrid beam-column members can be found in the recent research (Liu 2009). Another interested point may be that the semi-rigid axial and shear connection models have been introduced in the nonlinear analysis method aforementioned.

This article discusses the connection models that are commonly applied in practice, the relationship between them, and their physical/mathematical meaning. The characteristics of the empirical power models are discussed at first, and then an extended four-parameter model is proposed to simulate the behavior of connections. After presenting a simple analysis method to estimate the model parameters, the methods of linear and nonlinear regression analyses on the basis of the modified Levenberg-Marquardt and the separable nonlinear least-square methods are provided to determine the required model parameters using observed datum pairs. Although this article presents the connection modeling focused on rotational behaviour, the discussed models can be applied in general to axial or shear connections.

2. Nonlinear moment-rotation models

Moment-rotation relationship of semi-rigid connections can be obtained through integrating the stresses in the connection region by analysis alone. It is difficult to achieve much more accurate results because the complicated stress-strain relationships over a connection. This is due to the uncertainty of the common mechanical properties such as Young's modulus E , Poisson's ratio ν , yield stress, and ultimate stress in the post-elastic range. These values for different materials in any material or design standard or handbook (e.g., AISC 2005) are averaged from coupon tests. To illustrate the inaccuracy involved in the analysis, the nonlinear behavior of the stress-strain relationship from an extreme simple tension test is discussed as described for mild steel in the literature (Hibbeler 2004). In the inelastic range up to rupture, the stress-strain relationship may be difficult to be determined from the recorded data due to the change of the cross-sectional area in the loading process. For instance, if a specimen has initial cross-sectional area A_0 and gauge-length distance l_0 between the two punch marks, the strain is defined as

$$\varepsilon = (l - l_0)/l_0 \quad (1)$$

where l is the instantaneous length under the action of axial force P . It should be pointed out that the length l in Eq. (1) is at the final state of deformation. If the instantaneous length should be considered such as in large deformation situations, however, the actual strain may be different from

that defined in Eq. (1). To distinguish the strain with and without accounting for the deformation process, the terminology of engineering strain is used in this subsection to refer to as the strain in Eq. (1), while the following strain is referred to as true strain

$$\varepsilon_{tr} = \int_{l_0}^l \frac{dl}{l} = \ln \frac{l}{l_0} = \ln(1 + \varepsilon) \quad (2)$$

which takes the deformation process into account. Note that the terminology of engineering and true stress/strain is not used in the engineering community, but stress/strain is employed frequently.

It is seen from Eqs. (1) and (2) that, the engineering strain ε is progressively greater than true strain ε_{tr} in tension but less in compression. At the same time, if the instantaneous cross-sectional area is defined as A , the true stress σ_{tr} and engineering stress σ have expressions $\sigma_{tr} = P/A$ and $\sigma = P/A_0$. If the material is assumed incompressible (i.e., $Al = A_0l_0$), the true stress and engineering stress have the following relationship

$$\sigma_{tr} = \sigma(1 + \varepsilon) = \sigma e^{\varepsilon_{tr}} \quad (3)$$

It can be seen from Eq. (3) that the true stress is increasingly higher than the engineering stress in tension but lower in compression. In engineering practice the true stress-strain curve is replaced by the engineering stress-strain curve when the strain is small. Such replacement is accurate slightly up to yield-stress point and the error after this point is ignored because it may not be of interest in general structure design. Note also that the assumption of $Al = A_0l_0$ may not hold in the range after necking or cracking. This indicates that even the true stress-strain relationship Eq. (3) may not correctly model the material behavior in the post-yielding range, especially when loading beyond the point of necking. Therefore, instead of using Eq. (3) empirical stress-strain functions (e.g., Ramberg-Osgood 1943, Richard-Abbott 1975) are employed to represent the σ - ε relationship to fit with experimental data.

Now, even if the previous nonlinear σ - ε relationships can be established for a fibre or a component within a joint or connection region, it may be difficult to derive the moment-rotation relationship of the connection by integrating all the stresses over the region due to the highly-nonlinear stress-strain distributions. Thus, the component-based joint modelling may involve much of uncertainty in modeling the nonlinear behaviour of each component. To reduce such uncertainty caused by the simplified analysis model, experimental data of the similar connections may be applied to verify and adjust the analytical modelling such that the accuracy of the analytical results is improved. This is beyond the scope of this article, and the following presentation is focused on the characteristics of the mathematic models, which can be applied to deal with either analytical or experimental data of semi-rigid connections.

2.1 Rotation-based relationship

The common models for moment-rotation relationships applied in engineering are illustrated in Fig. 2, where the actual curve in heavy-thick line obtained from experimental results can be represented by linear or piecewise linear or nonlinear curves. The linear relation 0-1-3 in Fig. 2(a) is the most popular model applied to the linear structural analysis for the serviceability limit states design. It can be seen that the linear relation is in a limited domain, and using such a linear model in structural analysis may lead to significant error but in conservative (Liu 2009). In order to improve the accuracy, the bilinear loading path 0-2-3-4-5 may be used when elastic deformation is

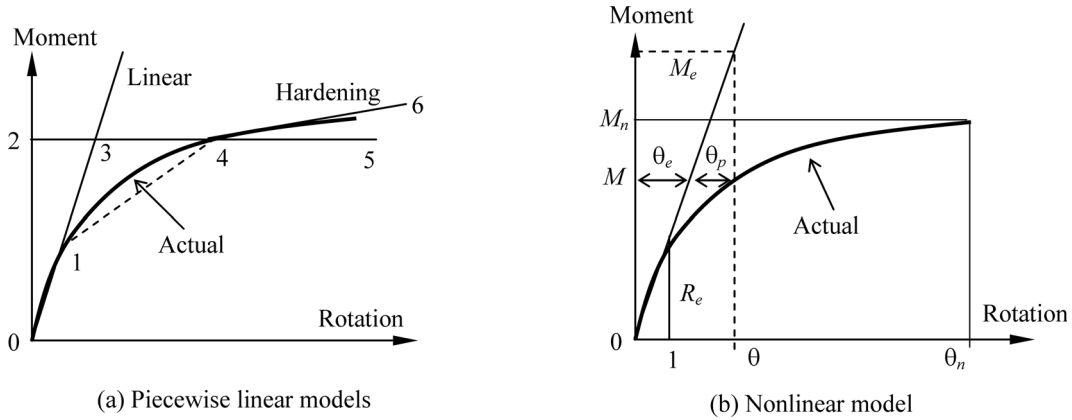


Fig. 2 Mathematical representations of the moment-rotation relations

negligibly small, while using bilinear loading path 0-1-3-4-5 takes the elastic deformation into account. To further reflect the actual behavior of connections, the trilinear 0-1-4-5 is more close to the actual $M-\theta$ relationship, whereas the trilinear 0-1-4-6 further includes the strain hardening effect.

The linear elastic model above is essential in conventional structural analysis and design, especially for preliminary assessment by hand calculation. While the bilinear or trilinear model is incorporated in a nonlinear analysis to assess the safety margin. For computer-based analysis, a more sophisticated nonlinear model may be considered in lieu of the bilinear or trilinear model. At first, it is assumed that the stress-strain power model (Ramberg and Osgood 1943) is used to model the actual moment-rotation relationship as shown in Fig. 2(b), where parameters θ , θ_e , θ_p , and R_e are the total rotation, elastic rotation, additional rotation and elastic rotational stiffness. For a given loading level M , the actual rotation θ can be considered the summation of elastic rotation θ_e and additional rotation θ_p and expressed as

$$\theta = \theta_e + \theta_p = \theta_e + \kappa\theta_e^\gamma = M/R_e + \kappa(M/R_e)^\gamma \tag{4}$$

where the three parameters R_e , κ and γ are determined using analytical/experimental data. Eq. (4) is of clear physical meaning that indicates the total deformation is nonlinearly scaled up by adding a nonlinear portion θ_p , which is expressed as a function of the elastic deformation θ_e by means of combination factor κ and exponent γ . Parameter γ is generally not equal to unity and its variation will adjust the curve shape. Thus, like the Ramberg-Osgood model, Eq. (4) is commonly called as a power law to simulate the constitutive relationship of connections. Once the elastic stiffness R_e is determined at first by experimental data, parameters κ and γ can be estimated using the linear least-square curve-fitting method through the following expression

$$\ln \kappa + \gamma \ln(M/R_e) = \ln(\theta - M/R_e) \tag{5}$$

Alternatively, the three parameters can be found from a nonlinear regression analysis using the method presented later. The advantage of the power model of Eq. (4) is that the model parameters can be readily determined using Eq. (5) for the experimental data of a semi-rigid connection.

Realize from Fig. 2(b) that the power model Eq. (4) is based on modifying the elastic deformation by adding an additional deformation term θ_p , and some information in the limit state, such as the nominal maximum moment M_n , is not directly reflected in the expression. Alternatively, the total

rotation θ may be reached by scaling up the linear elastic deformation θ_e by multiplying a non-dimensional term and this leads to

$$\theta = \frac{M/R_e}{[1 - (M/M_n)^\gamma]^{1/\gamma}} \quad (6)$$

where the ratio $M/M_n \leq 1$ allows for the linear elastic deformation to be amplified. Note that the exponent γ here has different meaning from that in Eq. (4). If moment M approaches nominal M_n in Eq. (6), the total deformation tends to infinity and the connection stiffness approaches zero. Eq. (6) is also referred to as a three-parameter power model, which has been applied to simulate the θ - M relation of semi-rigid connections (Chen *et al.* 1996). If the same set of data is used to determine the three parameters in each model of Eqs. (4) and (6), both the two models can be used to simulate the same connection behaviour.

2.2 Moment-based relationship

It may be convenient to express moment M as a function of rotation θ for the connections. From Eq. (6) the bending moment can be expressed in terms of rotation as

$$M = \frac{M_e}{[1 + (M_e/M_n)^\gamma]^{1/\gamma}} = \frac{R_e \theta}{[1 + (R_e \theta/M_n)^\gamma]^{1/\gamma}} \quad (7)$$

The physical meaning of the M - θ relationship of Eq. (7) can be interpreted through Fig. 3, where if specifying a rotation level θ , the actual moment M can be achieved by scaling down the linear moment $M_e (= R_e \theta)$ by a factor as shown in the equation. If a reference rotation $\theta_0 (= M_n/R_e)$ shown in Fig. 3 is introduced, the expression of Eq. (7) can be written in non-dimensional form as

$$\frac{M}{M_n} = \frac{\theta/\theta_0}{[1 + (\theta/\theta_0)^\gamma]^{1/\gamma}} \quad (8)$$

This expression may be used to eliminate the influence of dimensions of connections.

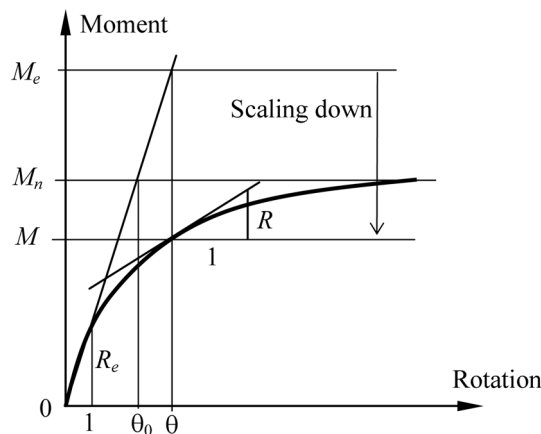


Fig. 3 Rotational stiffness based on the nonlinear model

2.3 Rotational stiffness

Upon differentiating Eqs. (7) or (8) with respect to θ , the tangent rotational stiffness R of the connection can be found as

$$R = \frac{dM}{d\theta} = \frac{R_e}{[1 + (\theta/\theta_0)^\gamma]^{1+1/\gamma}} \quad (9)$$

It is seen for the three-parameter model that tangent stiffness R of the connection degrades to zero when rotation θ tends to infinity for any positive value of exponent γ . This means that the three-parameter model Eq. (8) does not include strain hardening/softening effect and thus can only simulate some types of connections.

It may be concluded that the above nonlinear moment-rotation model of connections can be interpreted as the modification of the linear model by scaling up rotation or scaling down bending moment. For a given loading level, the actual rotation may be expressed as the linear elastic rotation plus an additional rotation (i.e., scaling up the elastic rotation). Inversely, for a given rotational loading level, the actual moment is obtained by scaling down the linear moment.

3. Moment-rotation model with four parameters

This section presents the derivation of the four-parameter connection model based on the three-parameter model discussed in the previous section. After discussing the nature of Richard-Abbott and Menegotto-Pinto models, a general four-parameter model is studied. In the end of this section, a guideline for establishing a hysteretic model is provided on the basis of the established connection model in monotonic loading.

3.1 Four-parameter model

In the three-parameter model when rotation θ becomes very large, the rotational stiffness R in Eq. (9) tends to zero, and strain hardening/softening behaviour is excluded in the model. If the strain hardening/softening is significant for the connections under consideration, a modified model should be developed. When a nominal stiffness R_n in the large rotation range in Fig. 4 is introduced to represent the strain hardening/softening behaviour, the stiffness R in Eq. (9) can be modified and expressed as

$$R = \frac{dM}{d\theta} = \frac{(R_e - R_n)}{[1 + (\theta/\theta_0)^\gamma]^{1+1/\gamma}} + R_n \quad (10)$$

which satisfies the following conditions: $R(0) = R_e$ and $R(\infty) = R_n$, and when $R_n = 0$ Eq. (10) reduces to Eq. (9). Integrating Eq. (10) with respect to θ once yields the following moment

$$M = \frac{(R_e - R_n)\theta}{[1 + (\theta/\theta_0)^\gamma]^{1/\gamma}} + R_n\theta \quad (11)$$

To be consistent with Eq. (8), the reference rotation θ_0 is taken as

$$\theta_0 = M_0/(R_e - R_n) \quad (12)$$

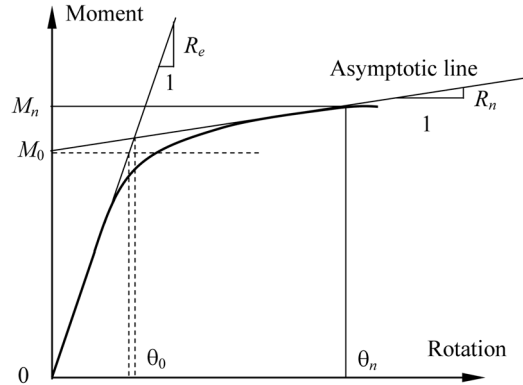


Fig. 4 Four-parameter power models with different references

which represents the rotation at the intersection between tangent line associated with elastic stiffness R_e and the line with nominal stiffness R_n indicated in Fig. 4. In Eq. (12) M_0 is referred to as a reference moment. Substituting Eq. (12) into Eq. (11) yields the following moment-rotation relationship

$$M = \frac{(R_e - R_n)\theta}{\{1 + [(R_e - R_n)\theta/M_0]^\gamma\}^{1/\gamma}} + R_n\theta \quad (13)$$

which is same as the moment-rotation model or stress-strain model proposed by Richard and Abbott (1975). In addition to the notations previously defined in Fig. 3, the parameter R_n is referred to as the nominal strain-hardening/softening stiffness, while parameter γ still controls the shape of the curve so that it is referred to as a shape parameter.

3.2 Characteristics of four-parameter model

It is seen from Fig. 4 that for the four-parameter model, the relation between reference moment M_0 and nominal maximal moment M_n is given by

$$M_0 = M_n - R_n\theta_n \quad (14)$$

which is equivalent to Eq. (12) but the nominal rotation θ_n rather than the reference rotation θ_0 is addressed. If set R_n to 0, Eq. (13) reduces to Eq. (7) and the reference moment M_0 takes the same value of nominal moment M_n . From Eq. (10), the tangent stiffness tends to R_n instead of zero when rotation θ tends to infinity as shown in Fig. 4. Thus, positive R_n is associated with strain hardening, and negative associated with strain softening. It should be pointed out that using negative stiffness of connections may cause numerical problem in the structural analysis. Such a problem is not yet well resolved and using negative stiffness should be with caution. When $R_n = R_e$, the expression of Eq. (13) reduces to the following linear model

$$M = R_e\theta \quad (15)$$

It can be also shown that if the shape parameter γ in Eq. (13) tends to infinity, the moment-rotation relationship of the four-parameter model reduces to

$$M = \begin{cases} R_e \theta & \text{if } \theta \leq \theta_0 \\ R_n \theta & \text{if } \theta > \theta_0 \end{cases} \quad (16a, b)$$

which corresponds to the bilinear model with trace 0-1-4 as shown in Fig. 2(a). If the asymptotic line of the model in Eq. (13) is assumed as M_a , the asymptotic line of the four-parameter model can be expressed as

$$M_a = M_0 + R_n \theta \quad (17)$$

which is indicated in Fig. 4, and is derived from the conditions $M(\theta) - M_a(\theta) \rightarrow 0$ and $M(\theta)/M_a(\theta) \rightarrow 1$. It is seen that the reference moment M_0 is equal to the moment $M_a(\theta)$ when θ is equal to zero, while nominal maximum moment is attained from Eq. (17) when θ is equal to θ_n . All the previous discussions indicate that the four-parameter model can simulate linear, bilinear, and highly nonlinear behavior of moment-rotation relationships with appropriate parametric values. This model has been selected to model the behaviour of semi-rigid connections (Hsieh and Delerlein 1990, Xu 1994, Faella *et al.* 2000, Kishi *et al.* 2004, Liu *et al.* 2008).

3.3 Generalized four-parameter model

It is interesting to note that a similar expression of a four-parameter model proposed by Menegotto and Pinto (1973) is used to simulate the behaviour of reinforcement bars in the nonlinear analysis of reinforced concrete frameworks subjected to cyclic loading. This model has been frequently employed in the area of reinforced concrete structures to represent the nonlinear monotonic stress-strain relationship of steel reinforcement (Faria *et al.* 2004). If Menegotto-Pinto model is selected to simulate connections, the mathematic moment-rotation relationship can be expressed using the notations in this article as

$$M = \frac{(R_e - R_n) \theta}{[1 + (R_e \theta / M_0)^\gamma]^{1/\gamma}} + R_n \theta \quad (18)$$

which is similar in form to that in Eq. (13). When the reference moment M_0 is taken the same value as that in Richard-Abbott model, the only difference between these two models is the reference rotation θ_0 as shown in Fig. 4. For Menegotto-Pinto model, the reference rotation θ_0 corresponding to Eq. (18) can be expressed as

$$\theta_0 = M_0 / R_e \quad (19)$$

which is the rotation at the intersection of elastic tangent line and line $M = M_0$ shown in Fig. 4. It is observed that for the same reference moment M_0 , both reference rotations in the two models are quite close. Thus, when nominal stiffness R_n is generally far smaller than the elastic stiffness R_e , the difference between these two models is negligible small. In addition, the two four-parameter models reduce to the three-parameter model of Eq. (7) as shown in the previous derivation when R_n tends to zero.

In the Richard-Abbott and Menegotto-Pinto models, the reference M_0 or reference rotation θ_0 is used to characterize model behavior. The reference rotation θ_0 can be used to show the sharp turning point of the curve as shown in Fig. 4. If a new parameter ρ , taken as the reciprocal of the reference rotation θ_0 , is introduced so that a generalized four-parameter is reached

$$M = \frac{(R_e - R_n)\theta}{[1 + (\rho\theta)^\gamma]^{1/\gamma}} + R_n\theta \quad (20)$$

It is important to point out that parameter ρ is independent on the rest three parameters R_n , R_e and γ in the model of Eq. (20). Obviously, this model includes Richard-Abbott and Menegotto-Pinto models if $\rho = (R_e - R_n)/M_0$ and $\rho = R_e/M_0$, respectively.

For any given observed data to be fitted, different four parameters are obtained from the models in Eqs. (13), (18) or (20) by using regression analysis with least-square method (see the example in Subsection 5.1). However, much close predictions can be achieved through these models for the same datum pairs. As aforementioned the Menegotto-Pinto model proposed in 1973 has been extensively used in concrete structures to model the nonlinear stress-strain relationships of the reinforcements under cyclic or seismic loading. While the Richard-Abbott model is frequently used to simulate the nonlinear moment-rotation relations of semi-rigid connections of steel frameworks. Both of them can be used to model semi-rigid connections. The model in Eq. (20) may be applied in the analysis of both reinforced concrete and steel structures.

Compared with the Menegotto-Pinto and Richard-Abbott models, two benefits can be achieved by using the proposed model in Eq. (20). At first, the model of Eq. (20) is more flexible to be applied in nonlinear regression analysis, where the popular algorithm of separable nonlinear least squares (Golub and Pereyra 2003) can be used with two linear parameters R_n and R_e and two nonlinear parameters ρ and γ . In Menegotto-Pinto model only R_n is linearly separable parameter, while in Richard-Abbott model no parameter is linearly separable. Secondly, the reference moment M_0 is not implicitly involved in Eq. (20). Thus, a moment, such as the plastic moment M_p in inelastic analysis (Liu *et al.* 2008), can be selected to normalize the expression in Eq. (20).

3.4 Modeling of connections under cyclic loading

After Northridge earthquake, it is recognized that welded connections experienced unexpected damage and semi-rigid connections had favorable performance against earthquake ground motion. Welded connections behave more like rigid connections. To account for semi-rigid connections in seismic analysis of steel frames, hysteretic effect of connections should be modeled. In the past two decades, much of research is given to investigate the dynamic behavior of semi-rigid connections and the associated steel structures subject to cyclic or transient loading (Elnashai *et al.* 1998, Chan and Chui 2000, Simões *et al.* 2001, Pucinotti 2006, Yang and Kim 2007, Saravanan *et al.* 2009). The methods provided in the literature (Liu and Lu 2010) may be used to enforce base earthquake motions to the superstructures with semi-rigid connections.

Modeling of connections accounting for cyclic behavior can be achieved upon using the connection model for monotonic loading. The hysteretic behavior for the dynamic analysis should include the effect of loading, unloading, and reloading in cyclic loading process. The backbone curve in either positive or negative loading direction can be represented by such as Richard-Abbott connection model. In the positive loading direction, the moment-rotation relation follows the defined curve with elastic stiffness R_{e+} and nominal stiffness R_{n+} . Similarly, the moment-rotation relation follows the defined curve with elastic stiffness R_{e-} and nominal stiffness R_{n-} in the negative direction loading. Generally, the behavior of a connection in positive loading direction is different from that in the negative loading direction. Once the monotonic connection model in each loading direction is obtained, the corresponding hysteretic model can be established. More detailed information for the

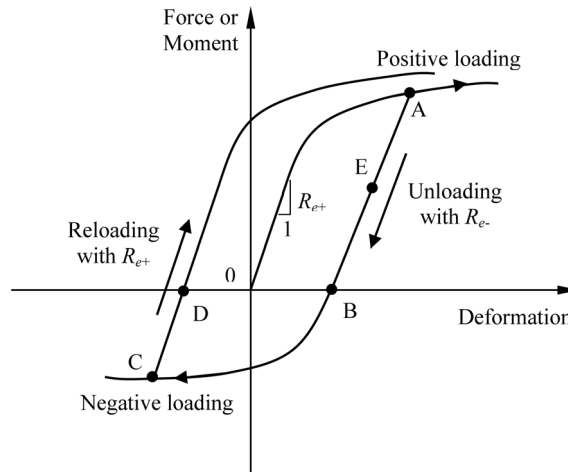


Fig. 5 Cyclic modeling of connections

cyclic connection models can be found in the literature (Chan and Chui 2000).

As a guideline for obtaining the cyclic model, Fig. 5 illustrates a way to model connections with cyclic behavior. Note that since axial connection, shear connection, and moment connection may be involved in a frame (Liu 2008), the cyclic modeling in Fig. 5 may represent the axial force-deformation, shear-deformation, and moment-rotation relations. It is assumed that the connection is loaded in the positive direction following the monotonic connection (backbone) curve up to point A, and then linear unloading with elastic stiffness R_{e-} proceeds to point B, at which the internal loading reduces to zero. This unloading continues from point B following the monotonic connection curve in the negative direction down to point C, and then linear reloading occurs with elastic stiffness R_{e+} defined for positive loading direction. The first cycle is ended at point D, where the internal force/moment approaches zero. A new cycle will start from this point, and the cyclic loading is repeated till the completeness of external loading. It should be pointed out that when R_{e+} is not equal to R_{e-} , the elastic linear stiffness should be changed when reversal loading occurs in the linear unloading or reloading process. For instance, stiffness R_{e+} should be used when reloading occurs at point E in the linear unloading process in Fig. 5.

Note that the hardening effect is included in the cyclic model discussed because stiffness R_n shown in Fig. 4 is taken into account. It is observed that pinching effect is significant from experimental results. However, as indicated in the analysis against progressive collapse (Liu *et al.* 2010), the localised failure or stiffness degradation model may affect the localised response significantly but not the global response of the frame. Therefore, the hysteretic model described in Fig. 5 is considered sufficient to take the stiffness degradation of connections under cyclic/dynamic loading into account.

4. Determination of model parameters

In principle, in order to obtain the parameters involved in any one of mathematical models discussed in Section 3, a linear or nonlinear regression analysis should be performed to fit the

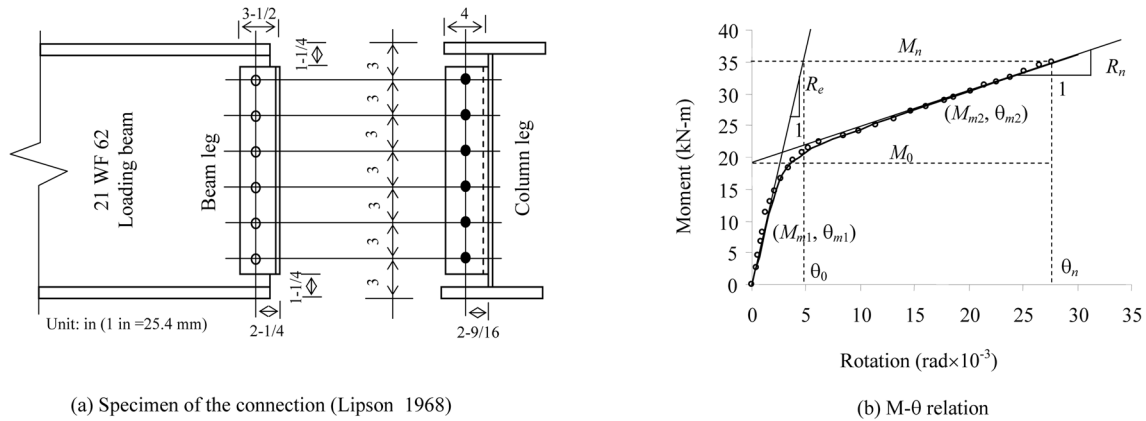


Fig. 6 Experimental data for multiple regression analysis

experimental or analytical data. For example, for a single-web angle connection (Lipson 1968) shown in Fig. 6(a), the experimental data are shown as the small circles in Fig. 6(b). The four parameters R_e , R_n , M_0 , and γ in Richard-Abbott model may be obtained using nonlinear least-square method. The standardized functions can be obtained for different type of connections by using multiple linear regression analysis (Attiogbe and Morris 1991). This section presents how to determine the parameters R_n , R_e , ρ , and γ in the modified four-parameter model in Eq. (20).

Note that because of the slip between components at the initial moment, some tested moment-rotation values may not represent the actual behavior of the connections. If necessary, these untrue values should be excluded prior to regression analysis.

4.1 Nonlinear regression analysis

A sophisticated way for finding the parameters in a mathematical model is to conduct a nonlinear regression analysis based on the given datum pairs. Using Richard-Abbott model and tested data, nonlinear least-square method was used to fit the data (Attiogbe and Morris 1991). Several algorithms can be used to estimate the parameters in either linear or nonlinear models. Since it is crucial to find the parameters in the model that is used in the analysis and design of frameworks, this section presents in much detail the methods for estimating model parameters. It is well known that the Gauss-Newton (GN) method employs the linearization of the fitting function to find the parameters by solving iteratively a linear least-square problem. To shrink the step size at each step to ensure a reduction in the summation of the squares, the modified Levenberg-Marquardt method adopts a trust-region approach, also referred to as ridge regression or regularization to find the parameters (Golub and Pereyra 2003).

Some software packages such as NL2SOL (Dennis *et al.* 1981) that uses a hybrid combination of GN method and estimation of a positive-definite approximation to the Hessian from differences of the first derivatives can be directly employed to conduct the nonlinear regression analysis. Some related information such as the updated variable projection (VP or VARPRO) method can also be found in the review article (Golub and Pereyra 2003). To determine the parameter values involved such as in the four-parameter model, the following moment-rotation model for semi-rigid connections is defined

$$M_j \approx F_j = \frac{(R_e - R_u)\theta_j}{[1 + (\rho\theta_j)^\gamma]^{1/\gamma}} + R_u\theta_j \quad (21)$$

where F_j is a function that fits the experimental or analytical datum pairs (M_j, θ_j) ($j = 1, 2, \dots, m$). Based on Eq. (21), the nonlinear regression analysis is required to solve the following minimum problem

$$\min_{(R_e, R_u, \rho, \gamma)} \sum_{j=1}^m \{M_j - F_j\}^2 \quad (22)$$

In regression analysis, the first derivatives of the fitting function F_j with respect to each of the parameters R_e , R_u , ρ , and γ are needed to form the Jacobian matrix in the analysis procedure such as in the Levenberg-Marquardt method. To simplify the expressions in the following derivation, let a parameter

$$\kappa_j = (\rho\theta_j)^\gamma \quad (23)$$

and then differentiating F_j with respect to each parameters yields

$$\frac{\partial F_j}{\partial R_u} = \theta_j - \frac{\theta_j}{(1 + \kappa_j)^{1/\gamma}} \quad (24a)$$

$$\frac{\partial F_j}{\partial R_e} = \frac{\theta_j}{(1 + \kappa_j)^{1/\gamma}} \quad (24b)$$

$$\frac{\partial F_j}{\partial \rho} = -\frac{(R_e - R_u)\kappa_j\theta_j}{\rho(1 + \kappa_j)^{1+1/\gamma}} \quad (24c)$$

$$\frac{\partial F_j}{\partial \gamma} = \frac{(R_e - R_u)\theta_j[(1 + \kappa_j)\ln(1 + \kappa_j) - \kappa_j\ln\kappa_j]}{\gamma^2(1 + \kappa_j)^{1+1/\gamma}} \quad (24d)$$

Incorporating the subroutine for calculating the residual vector $\{M_j - F_j\}$ base on Eq. (22) and for all the derivatives in Eqs. (24a,b,c,d) into the FORTRAN codes (MINPACK, see the web link in the reference), the four parameters can be found. In order to compare the results between the Richard-Abbott, Menegotto-Pinto, and the proposed models, the derivatives related to Richard-Abbott and Menegotto-Pinto models with respect to the corresponding parameters are given in Appendix A. In these equations, parameter κ_j in each model has its own definition.

If the separable nonlinear least-square method is used, the function in Eq. (21) is rearranged and expressed as

$$M_j \approx F_j = R_e\Phi_1 + R_u\Phi_2 \quad (25)$$

where R_e and R_u are two linear parameters, while the two nonlinear functions Φ_1 and Φ_2 are given by

$$\Phi_1 = \frac{\theta_j}{[1 + (\rho\theta_j)^\gamma]^{1/\gamma}}, \quad \Phi_2 = \theta_j - \Phi_1 \quad (26a, b)$$

in which ρ and γ are two nonlinear parameters. In the nonlinear regression analysis, the first derivatives of the combination functions Φ_1 and Φ_2 with respect to each of the nonlinear parameters ρ and γ are needed, and the corresponding expressions are

$$\frac{\partial \Phi_1}{\partial \rho} = -\frac{\partial \Phi_2}{\partial \rho} = -\frac{\kappa_j \theta_j}{\rho(1 + \kappa_j)^{1+1/\gamma}} \quad (27a)$$

$$\frac{\partial \Phi_1}{\partial \gamma} = \frac{\partial \Phi_2}{\partial \gamma} = \frac{\theta_j[(1 + \kappa_j)\ln(1 + \kappa_j) - \kappa_j \ln \kappa_j]}{\gamma^2(1 + \kappa_j)^{1+1/\gamma}} \quad (27b)$$

where κ_j is given in Eq. (23). Comparing the algorithm of the foregoing separable nonlinear least-square method with that of the Levenberg-Marquardt method, the linear parameters are eliminated in the nonlinear iterative procedure by solving the linear least-square problem based the Moore-Penrose generalized inverse (Dennis *et al.* 1981). Thus, the separable nonlinear least-square method is more efficient than the Levenberg-Marquardt method.

4.2 Simple method

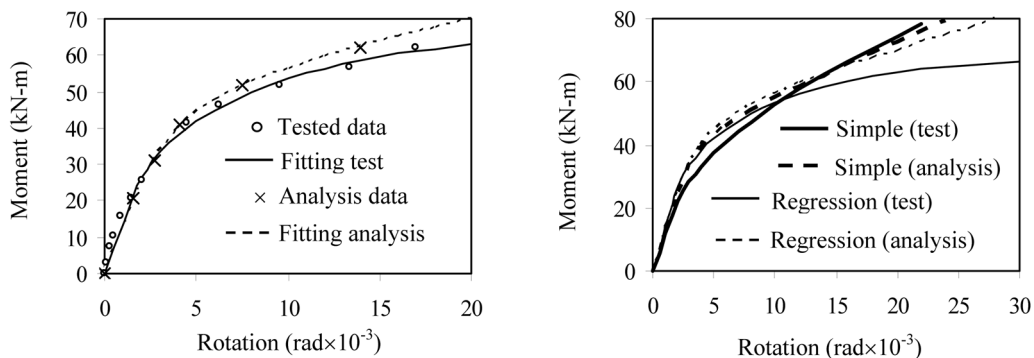
In view of the highly nonlinearity of the moment-rotation relationship, it is necessary to find a simple way that can quickly figure out the parameters by hand to approximately estimate the model parameters based on the observed data. In this regard, the following procedure may be useful.

From Fig. 7, the nominal maximum moment M_n and the corresponding rotation θ_n from the data to be fitted for a specific connection can be evaluated by

$$M_n = \frac{1}{m_0} \sum_j M_j; \quad \theta_n = \frac{1}{m_0} \sum_j \theta_j \quad (28a, b)$$

where m_0 denotes the number selected to estimate the average values at which term M_n might represent the maximal moment well, and m_0 may take number of two or three. The elastic or initial connection stiffness R_e can be determined using the following expression

$$R_e = \frac{\sum_{j=3}^{m_1} M_j}{\sum_{j=3}^{m_1} \theta_j} \quad (29)$$



(a) Fitted curves with given data

(b) Comparisons of simple and regression analyses

Fig. 7 Moment-rotation curves from simple and regression analyses

where number m_1 is selected such that the moment M and θ have the best linear relationship in the elastic range. This can be generally determined from the first pairs of experimental data. Note that to get rid of the effect of initial slip between components, the first two to five datum pairs may be omitted, thus number of 3 suggested in Eq. (29) may change. Once the nominal maximum moment M_n and linear stiffness R_e are found, the parameter ρ associated with reference rotation can be determined by Eq. (20). To this end, the nominal stiffness R_n can be determined using the following formula

$$R_n = \frac{M_n - \sum_{k=1}^{m_2} M_k/m_2}{\theta_n - \sum_{k=1}^{m_2} \theta_k/m_2} = \frac{M_n - M^*}{\theta_n - \theta^*} \quad (30)$$

where the nominal point (M_n, θ_n) is known and taken as a reference point, and (M^*, θ^*) is the point obtained by taking the average of the appropriate m_2 datum pairs. These data, which are before or after but not included the data used in Eqs. (28a,b), will be chosen such that the moment M and θ have the best linear relationship in the domain close to the ultimate point. Note that back m_2 datum pairs are used in strain hardening case from the nominal point, while forward m_2 pairs are used in strain softening case. Once M_n , θ_n , and R_n are determined, Eq. (14) is used to find moment M_0 , and the corresponding reference rotation θ_0 is determined using Eq. (12) as defined for the Richard-Abbott model with the known elastic stiffness R_e and moment M_0 . Finally, to determine the shape parameter, Eq. (20) can be expressed as

$$\gamma = \ln[1 + (\rho\theta_j)^\gamma] / \ln\left[\frac{(R_e - R_u)\theta_j}{M_j - R_u\theta_j}\right] \quad (31)$$

If selecting a pair of (M_j, θ_j) such that $\theta_j = 1/\rho = \theta_0$, then the foregoing expression becomes

$$\gamma = \ln 2 / \ln\left[\frac{(R_e - R_u)\theta_0}{M_j - R_u\theta_0}\right] \quad (32)$$

where linear interpolation may be performed to determine M_j by using the known data. It is seen that the foregoing procedure is quite simple and only a calculator may be used to find the four parameters. The approximate values found through Eqs. (29) to (32) together with Eq. (19) can be served as the initial parameters used in the nonlinear regression analysis, and the application will be illustrated in the next section.

5. Example case studies

This section presents four examples that serve as the application of the connection models discussed above. Only the models for monotonic loading conditions are considered, and the hysteretic model will be incorporated into the analysis of structures. In the first example, the experimental data are used to compare the difference of connection models, and the second example is to compare the modeling with both experimental and analytical data. The third example is to show how the experimental curves are represented by the Richard-Abbott model. Finally, a discussion of model transformation is performed to transfer the moment-rotation curves expressed

by 3-parameter model into the curves expressed by 4-parameter model.

5.1 Modeling by experimental datum pairs

To illustrate the application of the foregoing procedure proposed in Section 4.2, the experimental data listed in the first two columns in Table 1 (Lipson 1968) are employed in the regression analysis. These tested results are obtained for the single-web angle connection in Fig. 6(a), where the original English units are shown in the figure. For the structural steel, the Young's modulus and yield stress are 200 GPa and 248 MPa, respectively. When using the Levenberg-Marquardt method, the following initial parameters for the three models are obtained from the formulas of the previous

Table 1 Experimental and predicted results

Experimental Data		Richard-Abbott		Menegotto-Pinto		Proposed	
θ (rad $\times 10^{-3}$)	M (kN-m)	M (kN-m)	Error (%)	M (kN-m)	Error (%)	M (kN-m)	Error (%)
0.00	0.00	0	0	0	0	0	0
0.40	2.75	3.46	25.49	3.46	25.50	3.46	25.49
0.53	4.66	4.59	-1.53	4.59	-1.52	4.59	-1.53
0.80	6.78	6.79	0.13	6.79	0.14	6.79	0.13
0.93	8.26	7.84	-5.13	7.84	-5.12	7.84	-5.13
1.33	11.23	10.72	-4.56	10.72	-4.56	10.72	-4.56
1.73	12.92	13.10	1.39	13.10	1.39	13.10	1.39
2.13	14.62	14.99	2.56	14.99	2.55	14.99	2.56
2.67	16.53	16.86	2.02	16.86	2.02	16.86	2.02
3.33	18.22	18.46	1.33	18.46	1.33	18.46	1.33
3.87	19.49	19.38	-0.58	19.38	-0.58	19.38	-0.58
4.67	20.76	20.41	-1.72	20.41	-1.72	20.41	-1.72
5.20	21.40	20.95	-2.08	20.96	-2.08	20.95	-2.08
6.27	22.46	21.87	-2.61	21.87	-2.61	21.87	-2.62
8.40	23.31	23.38	0.33	23.38	0.33	23.38	0.32
9.87	24.15	24.32	0.69	24.32	0.69	24.32	0.68
11.47	25.00	25.30	1.21	25.31	1.22	25.30	1.21
13.07	26.06	26.27	0.80	26.27	0.80	26.27	0.80
14.67	27.12	27.22	0.38	27.22	0.38	27.22	0.38
16.13	27.97	28.09	0.44	28.09	0.44	28.09	0.44
17.73	28.82	29.03	0.76	29.03	0.76	29.03	0.76
18.67	29.45	29.58	0.45	29.58	0.45	29.58	0.45
20.13	30.30	30.44	0.48	30.44	0.48	30.44	0.48
21.47	31.36	31.22	-0.43	31.22	-0.42	31.22	-0.42
22.53	31.78	31.85	0.21	31.85	0.21	31.85	0.21
23.87	32.63	32.63	0.00	32.63	0.00	32.63	0.00
25.07	33.48	33.33	-0.44	33.33	-0.43	33.33	-0.43
26.53	34.43	34.19	-0.70	34.19	-0.70	34.19	-0.70
27.60	34.96	34.81	-0.42	34.81	-0.42	34.81	-0.42

simple analysis. From Eqs. (28a,b) and Table 1, the nominal maximum moment and rotation can be found to be

$$M_n = (33.33 + 34.19 + 34.81)/3 = 34.29 \text{ kN-m}$$

$$\theta_n = (25.07 + 26.53 + 27.60) \times 10^{-3}/3 = 26.40 \times 10^{-3} \text{ rad}$$

According to Eq. (29), taking the first two non-zero datum pairs, the elastic stiffness is

$$R_e = \frac{4.66 + 6.78}{0.53 + 0.80} \times 10^3 = 8.581 \times 10^3 \text{ kN-m/rad}$$

To find the nominal stiffness, the three datum pairs close to those used to calculate the nominal maximum moment and rotation are selected from Table 1 and the corresponding average values are given by

$$M^* = (27.97 + 28.82 + 29.45)/3 = 28.74 \text{ kN-m}$$

$$\theta^* = (16.13 + 17.73 + 18.67) \times 10^{-3}/3 = 17.51 \times 10^{-3} \text{ rad}$$

Substituting the relevant values into Eq. (30) yields

$$R_n = \frac{M_n - M^*}{\theta_n - \theta^*} = \frac{34.29 - 26.40}{28.74 - 17.51} \times 10^3 = 0.6237 \times 10^3 \text{ kN-m/rad}$$

In order to determine the shape parameter γ , the reference moment M_0 is found as,

$$M_0 = M_n - R_n \theta_n = 34.29 - 0.6327 \times 10^3 \times 26.40 \times 10^{-3} = 17.587 \text{ kN-m}$$

and the corresponding reference rotation θ_0 from Eq. (12) is given by,

$$\theta_0 = \frac{M_0}{R_e - R_n} = \frac{17.587}{8.581 - 0.6237} \times 10^{-3} = \frac{17.587}{8.581 - 0.6237} \times 10^{-3} = 2.24 \times 10^{-3} \text{ rad}$$

From Table 1, the moment M_j can be determined by interpolation method as

$$M_j = 14.26 + (16.53 - 14.62) \frac{2.24 - 2.13}{2.67 - 2.13} = 15.03 \text{ kN-m}$$

Therefore, the shape parameter is found from Eq. (32) as,

$$\gamma = \ln 2 / \ln \left[\frac{(R_e - R_n) \theta_0}{M_j - R_n \theta_0} \right] = \ln 2 / \ln \left[\frac{(8.581 - 0.6237) \times 2.24}{15.03 - 0.6237 \times 2.24} \right] = 2.555$$

All the previous parametric values are listed in Table 2.

To illustrate the results from the proposed method of nonlinear regression analysis, the model parameters of the Richard-Abbott, Menegotto-Pinto, and the general models are determined using the approximate parameters calculated above. After conducting nonlinear-regression analysis for each connection model are the four parameters are found and listed in Table 2. It is seen from this table that the simple method can get well estimates of the model parameters for this example. There is no significant difference of the parameter R_e , R_n , or γ predicted by the three models, but the reference moment M_0 does have difference due to the distinction of the three models. As expected,

Table 2 Four parameters obtained using different models

Method	R_n (kN-m $\times 10^3$ /rad)	R_e (kN-m $\times 10^3$ /rad)	γ	M_0 (kN-m)	ρ (10^3 /rad)
Proposed (Simple)	0.6237	8.5809	2.5549	17.823	0.4465
Richard-Abbott	0.5832	8.6730	2.6054	18.729	-
Menegotto-Pinto	0.5831	8.6736	2.6046	20.080	-
Proposed (regression)	0.5831	8.6743	2.6036	-	0.4320

using Eq. (12) and the value ρ ($=1/\theta_0$) can yields $M_0 = 18.726$ kN-m, which is the value found in Richard-Abbott model, while using Eq. (19) $M_0 = 20.078$ kN-m, which is the value found in Menegotto-Pinto model. This shows that the proposed general model in this study can accurately cover the Richard-Abbott and Menegotto-Pinto models.

Applying the parameters in Table 2 to the corresponding models, the predicted moments for each model against the rotations are also listed in Table 1, where little difference of moments is found among the three models. The corresponding three moment-rotation curves are shown in Fig. 6(b) as the solid curves, which are concurrent. This indicates that all three four-parameter can efficiently simulate the test results.

If separable nonlinear least-square method is used, the linear parameters are found to be $R_e = 8.6733$ kN-m $\times 10^3$ /rad, and $R_n = 0.5831$ kN-m $\times 10^3$ /rad; while the nonlinear parameters $\rho = 0.4319$ 10^3 /rad and $\gamma = 2.6050$. These values are very close to those listed in Table 2. Note that the FORTRAN codes developed in this study based on Levenberg-Marquardt method can only be applied to the problem with one independent variable, whereas those codes based on separable nonlinear least-square method can deal with multiple independent variables.

5.2 Modeling by experimental and analytical data

This example is to check the effectiveness of the four-parameter model by means of the simplified method and nonlinear regression analyses through the use of the data presented by Sherbourne and Bahaari (1997). The experimental data for the connection are shown as the small circles, while the results obtained by the 3D finite element method are those shown as the cross symbols in Fig. 7(a). The four parameters obtained by using the simplified analysis method are shown in the second row of Table 3 for the experimental data. Taken these approximate parameters as the initial values in the nonlinear regression analysis for the same data, after conducting the nonlinear regression analysis the four parameters are shown in the third row of Table 3. Performing the same analyses for the data obtained from 3D finite element analysis, the four parameters are shown in the fourth and fifth

Table 3 Parameters in different models

Parameters		R_n (kN-m $\times 10^3$ /rad)	R_e (kN-m $\times 10^3$ /rad)	γ	ρ (10^3 /rad)
Test	Simple	1.3636	25.962	0.3491	0.6342
	Regression	-0.3305	30.596	0.2853	0.6405
3D	Simple	1.6827	13.454	2.5817	0.3052
	Regression	1.1673	14.261	2.0532	0.2763

columns, respectively.

It is seen from Table 3 that the nominal stiffness R_n is negative (-0.3305) from the regression analysis based on the experimental data shown in Fig. 7(a). This means that strain-softening behaviour will be predicted using the nonlinear regression analysis, while based on the simple analysis strain-hardening behaviour will be predicted. This phenomenon reminds us that sufficient experimental data located around the limit state should be used in the regression analysis so that the four parameter model can reflect actual moment-rotation behaviour. Using the obtained parameters, the curves from regression analyses are plotted in Fig. 7(a). It is seen that the four-parameter model can fit well both the experimental and the analytical data in the ranges of the given data, respectively. It is again show from Table 3 that the proposed simple method can lead to reasonably accurate results compared to those from nonlinear regression analysis. These curves are graphically shown in Fig. 7(b).

It should be pointed out that when using the four parameter model to fit either the experimental or analytical data, only the predictions within the original datum range are reliable. Significant errors may occur beyond the original datum domain. To improve the accuracy, the obtained data from either test or analysis should include the information of strain hardening/softening behaviour. Otherwise, significant error may occur in the nonlinear analysis of the framework with these connections when the rotations exceed datum ranges.

5.3 Modeling by experimental curves

Sometimes, the behavior of semi-rigid connections is characterized by moment-rotation curves rather than datum pairs, and the connection curves may be required to be digitized and then represented by a proper connection model for structural analysis. This example shows how the connection curves are transformed and represented using the Richard-Abbott four-parameter model on the basis of the tests of beam-to-column and column-to-base connections to be applied in the testing of semi-rigid portal frames (Liew *et al.* 1997). More detailed information regarding the specimen description, setup, dimensions, and material properties of the connections can be found in the referred paper.

The beam-to-column connection JSRF2 with bolted angles is considered in this example study, and the deformed connection associated with moment M and rotation angle θ are illustrated in Fig. 8(a), where the tested moment-rotation results for the connection are traced as the dotted curve. It is observed that the unloading and reloading behavior in the elastic range is consistent with that in the cyclic model shown in Fig. 5. In principle, the procedure for determining the model parameters is the same as that described in Subsection 5.1, but the tested curve should be digitized as the datum pairs as those in Table 1. Note also that the data in unloading and reloading are excluded, i.e., only the data relevant to the backbone curve are used. After applying the curve-fitting technique, the four parameters in Eq. (13) are determined to be $M_0 = 79$ kN-m, $R_e = 7202$ kN-m/rad, $R_n = 144$ kN-m/rad, and $\gamma = 0.57$. The corresponding curve is shown in Fig. 8(a) as the solid line, which is a good fitting with the tested data.

To be consistent with the JSRF2 connection that was used in the same frame, the tested column-to-base connection CB2 with axial force $0.24P_y$, where P_y is yield force in pure axial loading, is considered to obtain the four parameters in the Richard-Abbott model. The setup of the specimen associated with moment M and rotation angle θ are illustrated in Fig. 8(b), and the value of θ is determined using the end displacements D_1 and D_2 of the steel bars welded to the column and the

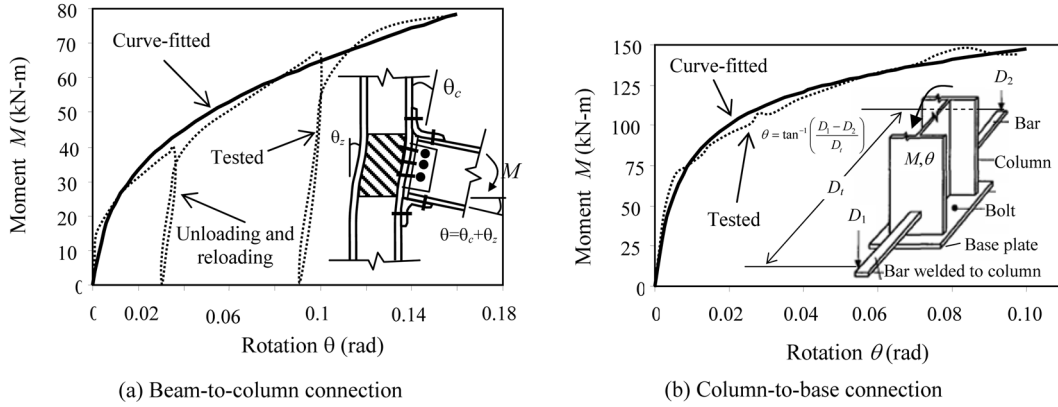


Fig. 8 Moment-rotation relations from experimental curves

total length D_1 of the two bars (Liew *et al.* 1997). The tested moment-rotation results for the connection are traced in Fig. 8(b) as the dotted curve. After applying the curve-fitting technique for the tested data, the four parameters in Eq. (13) are determined to be $M_0 = 148$ kN-m, $R_e = 24721$ kN-m/rad, $R_n = 151$ kN-m/rad, and $\gamma = 0.78$, which correspond to the solid curve shown in Fig. 8(b). Both the beam-to-column and column-to-base connection curves with the four-parameter model have been used in the nonlinear analysis of the portal frame (Liu *et al.* 2008).

5.4 Model transformation

Different nonlinear connection models discussed above in this article, including Ramberg-Osgood, Richard-Abbott, Menegotto-Pinto, and the general model, may be applied in the nonlinear analysis of steel structures connected with semi-rigid connections. Occasionally, transformation between different connection models may be required for a specific purpose of analysis. For example, in the nonlinear or progressive-collapse analysis of steel frames with semi-rigid connections (Liu 2009, Liu *et al.* 2010), the computer code has been developed on the basis of the Richard-Abbott model. If the computer code is used for the case where the connections are simulated by Ramberg-Osgood, then the connection curves represented by Ramberg-Osgood model have to be transformed into those characterized by the Richard-Abbott model such that the computer code can be directly applied. This example shows how such a model transformation is achieved using tested moment-rotation data of connections subjected to elevated temperature.

Involved in this example is to show the fire behavior of moment-rotation connections based on the tested results in the reference (Al-Jabri *et al.* 2005), and the connection curves expressed in 3-parameter (3-P) model are transformed to those expressed in 4-parameter (4-P) model for the purpose of structural analysis. In general, the behavior of moment-rotation connections under fire can be simulated using the Ramberg-Osgood 3-P model as

$$\theta = M/A + 0.01(M/B)^n \quad (33)$$

which is slightly different from that in Eq. (4), and here the three parameters n , A and B are determined using experimental results. On the basis of the model parameters for Group 2 connection as shown Fig. 9(a), the values of n , A and B are taken from the reference (Al-Jabri *et al.*

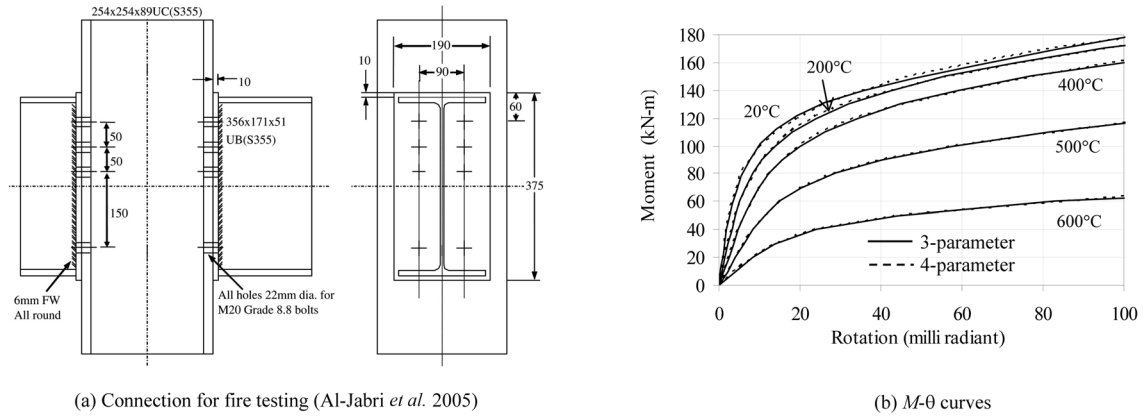


Fig. 9 Transformation from 3-Parameter to 4-Parameter Model

2005) and listed in Table 4 for the cases where the values of temperature are equal to 20°C, 200°C, 400°C, 500°C, and 600°C, respectively. Fig. 9(b) shows the corresponding $M-\theta$ curves of the connection as the solid lines.

At each temperature level, the $M-\theta$ data with sufficient pairs are calculated using Eq. (33), and then applying the curve-fitting technique as applied previously to obtain the four parameters in Eq. (13). For instance, when the ambient temperature is of 20°C, the four parameters are determined to be $R_e = 27323$ kN-m/rad, $R_n = 462.05$ kN-m/rad, $M_0 = 136.13$ kN-m, and $\gamma = 1.101$, which are shown in the second row of Table 4. For all other selected temperatures, the values of the four parameters are obtained similarly and listed in Table 4. Using Eq. (13) with the values of four parameters in Table 4, the 4-P connection curves are shown in Fig. 9(b) as the dashed lines. It is seen from the figure that the 3-P and 4-P models have very good agreement in modeling the moment-rotation relationship. These moment-rotation curves except for that in 500°C are applied in the analysis of steel frameworks to assess the fire behavior (Chen *et al.* 2010).

It is noted from Fig. 9(b) that the fire effect on steel connections is insignificant when the temperature is below about 200°C. Above this temperature, the influence of fire should be considered in the analysis, and how to incorporate such fire connections in the steel frameworks needs be investigated further. Note also that the fire behavior discussed is for the connection specimens that were put in the tests where the whole beam ends and column sections were put in a completely enclosed compartment. In reality, when a fire accident happens in an enclosed or partially-enclosed room space, only part of the connection/joint is exposed to fire. The connection behavior in this situation may be also interested for structural steel design.

Table 4 Parameters of 3-P and 4-P models in various temperatures

T (°C)	n	A (kN-m/mrad)	B (kN-m)	R_e (kN-m/rad)	R_n (kN-m/rad)	M_0 (kN-m)	γ
20	4.9	21.5	27.5	27323	462.05	136.13	1.101
200	4.9	13	27	15228	411.18	134.38	1.313
400	4.9	8.325	25.5	9022.4	453.83	117.86	1.689
500	4.9	5	18.65	5319	327.73	85.19	1.84
600	4.9	2.5	12.2	2635.6	180.38	46.05	1.931

6. Conclusions

Semi-rigid connection models for simulating the moment-rotation relationships are investigated in this article. Linear model is taken as a basis to derive the nonlinear connection models. It is shown that the Ramberg-Osgood (RO) model with three parameters is considered a linear term plus a nonlinear term that scales the elastic deformation up to the actual nonlinear deformation for a given bending moment level. This model can be alternatively expressed as a linear term plus a nonlinear term that scales the elastic bending moment down to the actual nonlinear moment for the given deformation level. To include more information in the ultimate state of a connection, the RO model can be extended to the four-parameter model such as the Richard-Abbott (RA) or Menegotto-Pinto (MP) model. A more general model, which includes RA and MP models, is proposed in this study to simulate the moment-rotation relationship of connections to facilitate nonlinear regression analysis. For preliminary analysis, a procedure is provided for determining the four parameters that approximately fit with the observed data. The modified Levenberg-Marquardt algorithm can be used to find the model parameters, but the separable nonlinear least-square algorithm is shown to be more effective for the proposed model compared to RA and MP models.

Analysis results show that the four-parameter connection model can well simulate linear, bilinear, and highly nonlinear moment-rotation relationships, especially for modeling the connections with significant strain hardening or softening. Note from this study that the predictions based on the connection models are dependent on the data used in the regression analyses. The predicted moment or rotation may not be accurate if it is far away from the connection data being used to establish the model. A guideline for developing a hysteretic model of connections subjected to cyclic loading is helpful for the analysis and design of steel structures under seismic loading. The hysteretic model of connections is generated using the established monotonic models in the positive and negative loading directions, and using the initial elastic stiffnesses for unloading and reloading. Example study also shows that the four-parameter model can be used to simulate the connections at high temperature.

Note that future work is needed to obtain the experimental or analytical data accounting for the variations of geometric size parameters for each category of connections so that the standardized model parameters can meet the requirements in practice. A series of standard experiments need to conduct to determine the connection parameters to be applied in the analysis and design of steel frameworks. Alternatively, the component-based method provided in the Eurocode 3 (CEN 2005) is attractive and can be effectively applied to establish the required connection modeling for design. In addition, modeling of axial and shear connections needs to be developed and the interaction of axial, shear, and bending effects should be taken into account.

References

- AISC (2005), *Specification for Structural Steel Buildings*, ANSI/AISC 360-05, American Institute of Steel Construction, Inc., Chicago, Illinois.
- Al-Jabri, K.S., Burgess, I.W., Lennon, T. and Plank, R.J. (2005), "Moment-rotation-temperature curves for semi-rigid joints", *J. Construct. Steel Res.*, **61**(2), 281-303.
- Attiogbe, E. and Morris, G. (1991), "Moment-rotation functions for steel connections", *J. Struct. Eng-ASCE*, **117**(6), 1703-1718.
- Barnett, T.C., Tizani, W. and Nethercot, D.A. (2001), "The practice of blind bolting connections to structural

- hollow sections: A review”, *Steel Compos. Struct.*, **1**(1), 1-16.
- Baniotopoulos, C.C. and Wald, F. (2000), *The Paramount Role of Joints into the Reliable Response of Structures*, Kluwer Academic Publishers, Dordrecht, The Netherlands.
- CEN (2005), *Eurocode 3: Design of Steel Structures, Part 1-8 – Design of Joints*, European Committee for Standardization, EN 1993-1-8, Brussels, Belgium.
- Chan, S.L. and Chui, P.P.T. (2000), *Non-linear Static and Cyclic Analysis of Steel Frames with Semi-rigid Connections*, Elsevier Science Ltd., Kidlington, Oxford, UK.
- Chen, K.M.G., Weckman, E.J., Liu, Y. and Grierson, D.E. (2010), “Analysis of steel frameworks subject to fire”, *Proceedings of the Sixth International Conference on Structures in Fire (SiF 10)*, Michigan, June.
- Chen, W.F., Goto, Y. and Liew, J.Y.R. (1996). *Stability design of semi-rigid frames*, John Wiley & Sons, Inc., New York.
- CSA-S16-09 (2009), *Design of Steel Structures*, National Standard of Canada, Canadian Standard Association, Mississauga, Ontario, Canada.
- Dennis, J.E., Gay, D.M. and Welsch, R.E. (1981), “Algorithm 573: NL2SOL—An adaptive nonlinear least-squares algorithm [E4]”, *ACM T. Math. Software*, **7**(3), 369-383.
- Elremaily, A. and Azizinamini, A. (2001), “Experimental behaviour of steel beam to CFT column connections”, *J. Construct. Steel Res.*, **57**(10), 1099-1119.
- El-Rimawi, J.A., Burgess, I.W. and Plank, R.J. (1997), “The influence of connections stiffness and behaviour of steel beams in fire”, *J. Construct. Steel Res.*, **43**(1-3), 1-15.
- Elnashai, A.S., Elghazouli, A.Y. and Denesh-Ashtiani, F.A. (1998), “Response of semi-rigid steel frames to cyclic and earthquake loads”, *J. Struct. Eng.*, **124**(8), 857-867.
- Faella, C., Piluso, V. and Rizzano, G. (2000), *Structural Steel Semi-rigid Connections-theory, Design and Software*, CRC Press, Boca Raton.
- Faria, R., Oliver, J. and Cervera, M. (2004), “Modeling material failure in concrete structures under cyclic actions”, *J. Struct. Eng-ASCE*, **130**(12), 1997-2005.
- FEMA-403 (2002), *World Trade Center Building Performance Study: Data Collection, Preliminary Observations and Recommendation*, Federal Emergency Management Agency (FEMA) Region II, New York, N.Y. USA.
- Frye, M.J. and Morris, G.A. (1975), “Analysis of flexibly connected steel frames”, *Can. J. Civil Eng.*, **2**(3), 280-291.
- Golub, G. and Pereyra, V. (2003), “Separable nonlinear least squares: the variable projection method and its applications”, *Inverse Probl.*, **19**, 1-26.
- Gong, Y. (2009), “Single-angle all-bolted shear connections”, *J. Construct. Steel Res.*, **65**(6), 1337-1345.
- Gong, Y. and Gillies, A. (2008), “Double-angle shear connections with short outstanding legs”, *Can. J. Civil Eng.*, **35**(8), 786-795.
- Goverdham, A.V. (1983), *A Collection of Experimental Moment-rotation Curves and Evaluation of Prediction Equations for Semi-rigid Connections*, Master’s Thesis, Vanderbilt University, Nashville, TN.
- Huber, G. (2001), “Semi-continuous beam-to-column joints at the Millennium Tower in Vienna, Austria”, *Steel Compos. Struct.*, **1**(2), 159-170.
- Kirby, B.R. (2001), “The behaviour of high-strength grade 8.8 bolts in fire”, *J. Construct. Steel Res.*, **33**(1-2), 3-37.
- Kishi, N. and Chen, W.F. (1986), *Data base of Steel Beam-to-column Connections*, Report No. CE-STR-86-26, School of Civil Engineering, Purdue University, West Lafayette, Indiana.
- Kishi, N., Komuro, M. and Chen, W.F. (2004), “Four-parameter power model for M- θ curves of end-plate connections”, *Proceedings of ECCS/AISC Workshop Connections in Steel Structures V: Innovative Steel Connections*, Amsterdam, The Netherlands, June.
- Kishi, N. and Chen, W.F. (1990), “Moment-rotation relations of semi-rigid connections with angles”, *J. Struct. Eng-ASCE*, **116**(7), 1813-1834.
- Krishnamurthy, N., Huang, H., Jeffrey, P.K. and Avery, L.K. (1979), “Analytical M- θ curves for end-plate connections”, *J. Struct. Div-ASCE*, **105**(1), 133-145.
- Hibbeler, R.C. (2004), *Statics and Mechanics of Materials*, 2nd Edition, Prentice-Hall, Inc., New Jersey.
- Hsieh, S.H. and Delerlein, G.G. (1990), “Nonlinear analysis of three-dimensional steel frames with semi-rigid connections”, *Comput. Struct.*, **41**(5), 995-1009.

- Langdon, G.S. and Schleyer, G.K. (2004), "Modelling the response of semi-rigid supports under combined loading", *Eng. Struct.*, **26**, 511-517.
- Lee, Y.L. and Melchers, R.E. (1986), "Moment-rotation curves for bolted Connections", *J. Struct. Eng-ASCE*, **112**(3), 615-635.
- Li, G.Q. and Guo, S.X. (2008), "Experiment on restrained steel beams subjected to heating and cooling", *J. Construct. Steel Res.*, **64**(3), 268-274.
- Liew, J.Y.W., Yu, C.H., Ng, Y.H. and Shanmugam, N.E. (1997), "Testing of semi-rigid unbraced frame for calibration of second-order inelastic analysis", *J. Construct. Steel Res.*, **41**(2/3), 159-195.
- Lipson, S.L. (1968), "Single-angle and single-plate beam framing connections", *Proceedings of the Canadian Structural Engineering Conference*, Canadian Steel Industries Construction Council, Canada.
- Liu, T.C.H. (1996), "Finite element modeling of behaviour of steel beam and connections in fire", *J. Construct. Steel Res.*, **36**(2), 181-199.
- Liu, Y. and Xu, L. (2005), "Storey-based stability analysis of multi-storey unbraced frames", *Struct. Eng. Mech.*, **19**(6), 679-705.
- Liu, Y., Xu, L. and Grierson, D.E. (2008), "Compound-element modelling accounting for semi-rigid connections and member plasticity", *Eng. Struct.*, **30**(5), 1292-1307.
- Liu, Y. (2009), "Hybrid member stiffness matrix accounting for geometrical nonlinearity and member inelasticity in semi-rigid frameworks", *Eng. Struct.*, **31**(12), 2880-2895.
- Liu, Y., Xu, L. and Grierson, D.E. (2010), "Influence of Semi-rigid Connections and local joint damage on progressive collapse of steel frameworks", *J. Comput. Aid. Civil Infrast. Eng.*, **25**(3), 184-204.
- Liu, Y. and Lu, Z. (2010), "Methods of enforcing earthquake base motions in seismic analysis of structures", *Eng. Struct.* (in press)
- Lui, E.M. and Chen, W.F. (1986), "Analysis and behaviour of flexibly-jointed frames", *Eng. Struct.*, **8**(2), 107-115.
- Menegotto, M. and Pinto, P. (1973), "Method of analysis for cyclically loaded reinforced concrete plane frames including changes in geometry and non-elastic behavior of elements under combined normal force and bending", *Proceedings of the IABSE Symposium on Resistance and Ultimate Deformability of Structures Acted on by Well-Defined Repeated Loads*, Final Report, Lisbon.
- MINPACK (1999), <http://www.netlib.org/minpack/>.
- Nethercot, D.A. (1985), "Utilization of experimentally obtained connection data in assessing the performance of steel frames", *Connection Flexibility and Steel Frames*, Ed. Chen, W.F., ASCE, Detroit.
- Nogueiro, P., Simões da Silva, L., Bento, R. and Simões, R. (2009), "Calibration of model parameters for the cyclic response of end-plate beam-to-column steel-concrete composite joints", *Steel Compos. Struct.*, **9**(1), 39-58.
- Pucinotti, R. (2006), "Cyclic mechanical model of semi-rigid top and seat and double web angle connections", *Steel Compos. Struct.*, **6**(2), 139-157.
- Richard, R.M. and Abbott, B.J. (1975), "Versatile elastic-plastic stress-strain formula", *J. Eng. Mech. Div.*, **101**(4), 511-515.
- Ramberg, W. and Osgood, W.R. (1943), "Description of Stress-strain curves by three parameters", Technical Note No. 902, National Advisory Committee for Aeronautics, Washington, D.C.
- Rathbun, J.C. (1936), "Elastic properties of riveted connections", *Trans.*, ASCE, **101**, 524-563.
- Sherbourne, A.N. and Bahaari, M.R. (1997), "Finite element prediction of end plate bolted connection behavior. I: Parametric study", *J. Struct. Eng-ASCE*, **123**(2), 157-164.
- Sakumoto, Y., Keira, K., Furumura, F. and Ave, T. (1993), "Tests of fire-resistance bolts and joints", *J. Struct. Eng.*, **119**(11), 3131-3150.
- Saravanan, M., Arul Jayachandran, S., Marimuthu, V. and Prabha, P., (2009), "Advanced analysis of cyclic behaviour of plane steel frames with semi-rigid connections", *Steel Compos. Struct.*, **9**(4), 381-395.
- Simões da Silva, L., de Lima, L.R.O., da S. Vellasco, P.C.G. and de Andrade S.A.L. (2004), "Behaviour of flush end-plate beam-to-column joints under bending and axial force", *Steel Compos. Struct.*, **4**(2), 77-94.
- Simões da Silva, L., Santiago, A., Vila Real, P. and Moore, D. (2005), "Behaviour of steel joints under fire loading", *Steel Compos. Struct.*, **5**(6), 485-513.
- Simões da Silva, L. (2008), "Towards a consistent design approach for steel joints under generalized loading", *J.*

- Construct. Steel Res.*, **64**(9), 1059-1075.
- Simões, R., Simões da Silva, L., Cruz, P., Wald, F. and Baniotopoulos, C.C. (1999), "Numerical modelling of column base connection", *Proceedings of COST C1 Conference Liège 1998*, Ed. Maquoi, R., Brussels.
- Xu, L. (1994), *Optimal Design of Steel Frameworks with Semi-rigid Connection*, Ph.D. Thesis, Department of Civil Engineering, University of Waterloo, ON, Canada.
- Yang, C.M. and Kim, Y.M. (2007), "Cyclic behaviour of beam-column connections in steel portals", *Proc. ICE., Struct. Build.*, **160**(5), 259-272.
- Zoetemeijer, P. (1983), *Proposal for Standardisation of Extended End Plate Connection based on Test results - Test and Analysis*, Rep. No. 6-83-23, Steven Laboratory, Delft.

Appendix

In order to compare the results obtained by different models, this appendix presents the first derivatives with respect to the parameters in Richard-Abbott (RA) model (1975) and Menegotto- Pinto (MP) model (1973) that are used in the nonlinear regression analysis based on the modified Levenberg-Marquardt algorithm to form the Jacobian matrix.

In Richard-Abbott model, the mathematic model of the relationship between moment M and rotation θ is given by

$$M = \frac{(R_e - R_u)\theta}{\{1 + [(R_e - R_u)\theta/M_0]^\gamma\}^{1/\gamma}} + R_u\theta \quad (\text{A1})$$

where parameters R_u , R_e , M_0 , and γ denote the nominal stiffness, elastic stiffness, reference moment, and shape parameter, respectively. If an intermediate parameter is introduced as

$$\kappa = \left[\frac{(R_e - R_u)\theta}{M_0} \right]^\gamma \quad (\text{A2})$$

upon differentiating M in Eq. (A1) with respect to each parameters yields

$$\frac{\partial M}{\partial R_u} = \theta - \frac{\theta}{(1 + \kappa)^{1+1/\gamma}} \quad (\text{A3a})$$

$$\frac{\partial M}{\partial R_e} = \frac{\theta}{(1 + \kappa)^{1+1/\gamma}} \quad (\text{A3b})$$

$$\frac{\partial M}{\partial M_0} = \left(\frac{\kappa}{1 + \kappa} \right)^{1+1/\gamma} \quad (\text{A3c})$$

$$\frac{\partial M}{\partial \gamma} = \frac{(R_e - R_u)\theta[(1 + \kappa)\ln(1 + \kappa) - \kappa\ln\kappa]}{\gamma^2(1 + \kappa)^{1+1/\gamma}} \quad (\text{A3d})$$

If the same notations for Richard-Abbott model are used, the Menegotto-Pinto (MP) model can be expressed as

$$M = \frac{(R_e - R_u)\theta}{[1 + (R_e\theta/M_0)^\gamma]^{1/\gamma}} + R_u\theta \quad (\text{A4})$$

If an intermediate parameter like in Eq. (A2) is used

$$\kappa = \left(\frac{R_e\theta}{M_0} \right)^\gamma \quad (\text{A5})$$

then differentiating M with respect to each parameters yields

$$\frac{\partial M}{\partial R_u} = \theta - \frac{\theta}{(1 + \kappa)^{1/\gamma}} \quad (\text{A6a})$$

$$\frac{\partial M}{\partial R_e} = \frac{\theta(R_e + R_u\kappa)}{R_e(1 + \kappa)^{1+1/\gamma}} \quad (\text{A6b})$$

$$\frac{\partial M}{\partial M_0} = \frac{(R_e - R_u)\theta\kappa}{M_0(1 + \kappa)^{1+1/\gamma}} \quad (\text{A6c})$$

$$\frac{\partial M}{\partial \gamma} = \frac{(R_e - R_u)\theta[(1 + \kappa)\ln(1 + \kappa) - \kappa\ln\kappa]}{\gamma^2(1 + \kappa)^{1+1/\gamma}} \quad (\text{A6d})$$